

# Deterministic SWAP gate using shortcuts to adiabatic passage

Yan Liang, Xin Ji, Hong-Fu Wang and Shou Zhang

Department of Physics, College of Science, Yanbian University, Yanji, Jilin 133002, People's Republic of China

E-mail: jixin@ybu.edu.cn

**Abstract.** We theoretically propose an alternative method to realize a deterministic SWAP gate using shortcuts to adiabatic passage based on the approach of Lewis-Riesenfeld invariants in cavity quantum electronic dynamics (QED). By combining Lewis-Riesenfeld invariants with quantum Zeno dynamics, the SWAP gate can be achieved deterministically. The strict numerical results show that our scheme is a fast and robust approach to achieve SWAP gate.

PACS numbers: 03.67.Lx, 42.50.-p, 42.50.Pq

*Keywords:* SWAP gate, shortcuts to adiabatic passage, quantum Zeno dynamics

## 1. Introduction

With the development of quantum science, the quantum computer replaces the universal computer just around the corner. The quantum logic gate is an indispensable part of the quantum computation. In quantum computing especially the calculation model of quantum circuit, the quantum logic gate is a basic operation of qubits quantum circuit. Recently, a number of schemes have been proposed to perform quantum logic gates and quantum information processing using optical devices [1], quantum dot [2, 3], QED systems [4], ion trap and superconducting devices [5, 8, 6, 7, 9]. As we know that a universal set of quantum operations can be constructed by a series of single- and two-qubit gates. Even though a multi-qubits gate could be decomposed into one- and two-qubit gates, it will be extremely complex and time-consuming in practical operation, that the arising decoherence will destroy the quantum system eventually. An efficient method of quantum information processing requires the whole operation is robust against the decoherence, easily prepared and measured. Adiabatic passage technique provides the robustness of the method against small variations of field parameters, and the decoherence caused by spontaneous emission can be avoided if the dynamics follows dark states, i.e. states without components on lossy excited states. However, that is not precise. If the controlling parameters do not change slowly enough, the transitions between different time-dependent instantaneous eigenstates may still exist, that the

fidelity of the evolved state with respect to the target one must be reduced. In other words, the adiabatic passage technique usually needs a long process [10]. If the required evolution time is too long, the speed of the system evolution will be slowed down, that the dissipation caused by decoherence, noise, and losses would destroy the expected dynamics finally.

Shortcuts to adiabatic passage is a promising technique for quantum information processing which actually fight against the decoherence, noise, or losses that are accumulated during a long operation time. Thus, a variety of schemes have been proposed to construct shortcuts to adiabatic passage in both theories and experiment [11, 12, 13, 14, 15, 16, 17, 18, 20, 21]. The shortcuts to adiabatic passage of logical gates operation have been presented, too. Chen *et al* [19] proposed a scheme of shortcuts to adiabatic passage for performing a  $\pi$  phase gate. And we have proposed a scheme of shortcut to adiabatic passage for constructing the multiqubit controlled phase gate [22].

In this paper, we effectively combine the advantages of shortcuts to adiabatic passage and quantum Zeno dynamic (QZD) [23, 24] to implement a SWAP gate. It dose not need the composition of element gates, but directly implements the deterministic SWAP gate through designing resonant laser pulses by the invariant-based inverse engineering. The logical SWAP gates in our scheme can be performed in a much shorter time than that based on adiabatic passage technique, and it is very robustness to the decoherence caused by atomic spontaneous emission and cavity decay.

This paper is structured as follows: In section 2, we give a brief description of the preliminary theory about Lewis-Riesenfeld invariants and QZD. In section 3, we effectively combine the shortcuts to adiabatic passage and QZD to implement the deterministic SWAP gate. Section 4 shows the numerical simulation results and feasibility analysis. The conclusion appears in section 5.

## 2. Preliminary theory

### 2.1. Lewis-Riesenfeld invariants

We first make a brief introduction of the Lewis-Riesenfeld invariants theory [25, 26]. Considering a system which is governed by a time-dependent Hamiltonian  $H(t)$ , and we can seek the time-dependent Hermitian invariants  $I(t)$  that is related to the original Hamiltonian  $H(t)$  to satisfy

$$i\hbar \frac{\partial I(t)}{\partial t} = [H(t), I(t)]. \quad (1)$$

Obviously, its expectation values remain constant all the time, and drives the system state evolve along the initial eigenstate of  $I(t)$ . For the time-dependent Schrödinger equation  $i\hbar \frac{\partial |\Psi(t)\rangle}{\partial t} = H(t)|\Psi(t)\rangle$ , the solution can be expressed by the superposition of dynamical modes  $|\Phi_n(t)\rangle$  of the invariants  $I(t)$

$$|\Psi(t)\rangle = \sum_n C_n e^{i\alpha_n} |\Phi_n(t)\rangle, \quad (2)$$

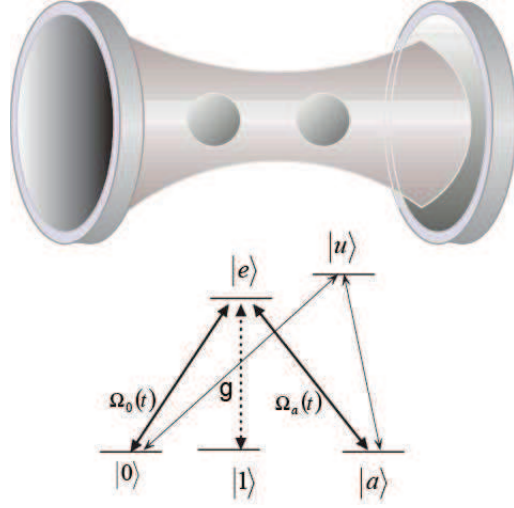


**Figure 1.** (Color online) The schematic setup of SWAP gate implementation. The atoms are trapped in a single mode optical cavity, and each atom possesses five atomic levels.

where  $n = 0, 1, \dots$ , and  $C_n$  is one of the time-independent amplitudes,  $\alpha_n$  is the Lewis-Riesenfeld phase.  $|\Phi_n(t)\rangle$  is one of the orthonormal eigenvectors of the invariant  $I(t)$  with the corresponding real eigenvalue  $\lambda_n$ , satisfying  $I(t)|\Phi_n(t)\rangle = \lambda_n|\Phi_n(t)\rangle$ . And the Lewis-Riesenfeld phase satisfies

$$\alpha_n(t) = \frac{1}{\hbar} \int_0^t dt' \langle \Phi_n(t') | i\hbar \frac{\partial}{\partial t'} - H(t') | \Phi_n(t') \rangle. \quad (3)$$

## 2.2. Quantum Zeno dynamics

The quantum Zeno effect was first proposed by Misra and Sudarshan, and it can be used to reduce the influence of the decoherence and dissipation by inhibiting the transition between quantum states through the frequent measurements [27]. We consider a system which is governed by the Hamiltonian

$$H_K = H_{\text{obs}} + KH_{\text{meas}}, \quad (4)$$

where  $H_{\text{obs}}$  is the Hamiltonian of the investigated quantum system and the  $H_{\text{meas}}$  is the interaction Hamiltonian performing the measurement.  $K$  is a coupling constant, and when it satisfies  $K \rightarrow \infty$ , the whole system is governed by the evolution operator

$$U(t) = \exp[-it \sum_n (K\lambda_n P_n + P_n H_{\text{obs}} P_n)], \quad (5)$$

where  $P_n$  is one of the eigenprojections of  $H_{\text{meas}}$  with eigenvalues  $\lambda_n$  ( $H_{\text{meas}} = \sum_n \lambda_n P_n$ ).

## 3. Shortcuts to adiabatic passage for the deterministic SWAP gate

We consider a system in which the atoms are fixed inside an optical cavity as shown in figure 1. Each atom possesses three ground states  $|0\rangle$ ,  $|1\rangle$ ,  $|a\rangle$  and two excited states  $|e\rangle$ ,

$|u\rangle$ . The transitions  $|0\rangle \leftrightarrow |e\rangle$  and  $|a\rangle \leftrightarrow |e\rangle$  are coupled to the laser pulses, with the corresponding Rabi frequencies  $\Omega_0(t)$  and  $\Omega_a(t)$ , respectively. The transition  $|1\rangle \leftrightarrow |e\rangle$  is strongly coupled to the single mode cavity field with the coupling constant  $g$ . And the auxiliary excited state  $|u\rangle$  is only used to implement the one-qubit operation.

Now we show the scheme to realize a deterministic SWAP gate. The initial state  $|\Psi_0\rangle$  of the two atoms and the cavity field is defined as

$$\begin{aligned} |\Psi_0\rangle = & \alpha_{00}|00\rangle_{AB}|0\rangle_C + \alpha_{01}|01\rangle_{AB}|0\rangle_C \\ & + \alpha_{10}|10\rangle_{AB}|0\rangle_C + \alpha_{11}|11\rangle_{AB}|0\rangle_C, \end{aligned} \quad (6)$$

where  $|nm\rangle_{AB}|0\rangle_C$  denotes atoms  $A$  and  $B$  are in the state  $|nm\rangle_{AB}$  ( $n, m = 0, 1$ ), and the cavity is in vacuum state  $|0\rangle_C$ .  $\alpha_{nm}$  denotes the amplitude of the state  $|nm\rangle_{AB}|0\rangle_C$ , and satisfies the normalization condition. The SWAP gate makes the values of the two qubits exchange and then the output state becomes

$$\begin{aligned} |\Psi\rangle = & \alpha_{00}|00\rangle_{AB}|0\rangle_C + \alpha_{01}|10\rangle_{AB}|0\rangle_C \\ & + \alpha_{10}|01\rangle_{AB}|0\rangle_C + \alpha_{11}|11\rangle_{AB}|0\rangle_C. \end{aligned} \quad (7)$$

There are three steps for the implementation of SWAP gate. First, we transfer the population of  $|01\rangle_{AB}|0\rangle_C$  to  $-|1a\rangle_{AB}|0\rangle_C$  completely with the help of laser pulses resonant with  $A$  atomic transition  $|0\rangle_A \leftrightarrow |e\rangle_A$  and  $B$  atomic transition  $|a\rangle_B \leftrightarrow |e\rangle_B$  with the corresponding Rabi frequencies  $\Omega_{0A}(t)$  and  $\Omega_{aB}(t)$ , respectively. After the interaction, the initial state becomes

$$\begin{aligned} |\Psi_1\rangle = & \alpha_{00}|00\rangle_{AB}|0\rangle_C - \alpha_{01}|1a\rangle_{AB}|0\rangle_C \\ & + \alpha_{10}|10\rangle_{AB}|0\rangle_C + \alpha_{11}|11\rangle_{AB}|0\rangle_C. \end{aligned} \quad (8)$$

Then the population of  $|10\rangle_{AB}|0\rangle_C$  is completely transferred to  $-|a1\rangle_{AB}|0\rangle_C$  with the similar method with the help of laser pulses resonant with  $B$  atomic transition  $|0\rangle_B \leftrightarrow |e\rangle_B$  and  $A$  atomic transition  $|a\rangle_A \leftrightarrow |e\rangle_A$  with the corresponding Rabi frequencies  $\Omega_{0B}(t)$  and  $\Omega_{aA}(t)$ , respectively. And the state of the system becomes

$$\begin{aligned} |\Psi_2\rangle = & \alpha_{00}|00\rangle_{AB}|0\rangle_C - \alpha_{01}|1a\rangle_{AB}|0\rangle_C \\ & - \alpha_{10}|a1\rangle_{AB}|0\rangle_C + \alpha_{11}|11\rangle_{AB}|0\rangle_C. \end{aligned} \quad (9)$$

Finally the population of the single atom state  $|a\rangle_{A(B)}$  is transferred into  $-|0\rangle_{A(B)}$  by the one-qubit operation with the help of the auxiliary excited state  $|u\rangle_{A(B)}$ , and the corresponding laser pulses are resonant with  $A(B)$  atomic transition  $|0\rangle_{A(B)} \leftrightarrow |u\rangle_{A(B)}$  and  $|a\rangle_{A(B)} \leftrightarrow |u\rangle_{A(B)}$  with the corresponding Rabi frequencies  $\Omega'_{aA(B)}(t)$  and  $\Omega'_{0A(B)}(t)$ , respectively. As a result, the state of the system turns into

$$\begin{aligned} |\Psi_3\rangle = & \alpha_{00}|00\rangle_{AB}|0\rangle_C + \alpha_{01}|10\rangle_{AB}|0\rangle_C \\ & + \alpha_{10}|01\rangle_{a1}|0\rangle_C + \alpha_{11}|11\rangle_{AB}|0\rangle_C, \end{aligned} \quad (10)$$

thus, the SWAP gate is obtained.

In the following, we show the details of how to realize the SWAP gate by combining the shortcuts to adiabatic passage and QZD. For the first step, the input laser pulses are resonant with  $A$  atomic transition  $|0\rangle_A \leftrightarrow |e\rangle_A$  and  $B$  atomic transition  $|a\rangle_B \leftrightarrow |e\rangle_B$  with

the corresponding Rabi frequencies  $\Omega_{0A}(t)$  and  $\Omega_{aB}(t)$ , respectively. The Hamiltonian of the first step in the interaction picture can be written as ( $\hbar = 1$ )

$$H_I = H_l + H_c, \quad (11)$$

$$H_l = \Omega_{0A}(t)|e\rangle_A\langle 0| + \Omega_{aB}(t)|e\rangle_B\langle a| + \text{H.c.}, \quad (12)$$

$$H_c = g_A a|e\rangle_A\langle 1| + g_B a|e\rangle_B\langle 1| + \text{H.c.}, \quad (13)$$

here  $a$  is the annihilation operator, and  $g_{A(B)}$  is the coupling strength between cavity mode and the trapped atom. In the following, we will set  $g_A = g_B$  for simplicity. Since the lasers do not couple with the atomic state  $|1\rangle$ , that the states  $|11\rangle_{AB}|0\rangle_C$  and  $|10\rangle_{AB}|0\rangle_C$  are decoupled from the other states in this step, and will not participate the evolution any more. For the state  $|00\rangle_{AB}|0\rangle_C$ , the evolution subspace can be spanned by the basis vectors  $|\varphi_1\rangle = |00\rangle_{AB}|0\rangle_C$ ,  $|\varphi_2\rangle = |e0\rangle_{AB}|0\rangle_C$ , and  $|\varphi_3\rangle = |10\rangle_{AB}|1\rangle_C$ . The Hamiltonian of this system reads

$$H_1 = \Omega_{0A}(t)|e\rangle_A\langle 0| + g_A|e\rangle_A\langle 1| + \text{H.c.} \quad (14)$$

For the condition  $g_A \gg \Omega_{0A}(t)$ , the Hilbert space is split into three invariant subspaces  $\Gamma_1 = |\varphi_1\rangle$ ,  $\Gamma_2 = \frac{1}{\sqrt{2}}(-|\varphi_2\rangle + |\varphi_3\rangle)$  and  $\Gamma_3 = \frac{1}{\sqrt{2}}(|\varphi_2\rangle + |\varphi_3\rangle)$  with the eigenvalues  $\lambda_1 = 0$ ,  $\lambda_2 = -g_A$ , and  $\lambda_3 = g_A$ . The corresponding projections are  $P_n^\alpha = |\alpha\rangle\langle\alpha|$  ( $|\alpha\rangle \in \Gamma_n, n = 1, 2, 3$ ). According to the QZD,  $U(t) = \exp[-it \sum_n (K\lambda_n P_n + P_n H_{\text{obs}} P_n)]$ , the effective Hamiltonian reduces to

$$H_{\text{eff}} = g_A|e\rangle_A\langle 1| + g_A|1\rangle_A\langle e|, \quad (15)$$

which indicates that the transition between  $|00\rangle_{AB}|0\rangle_C$  and  $|e0\rangle_{AB}|0\rangle_C$  is eliminated. For another state  $|01\rangle_{AB}|0\rangle_C$ , the system evolves in the subspace which is spanned by the basis vectors  $|\phi_1\rangle = |01\rangle_{AB}|0\rangle_C$ ,  $|\phi_2\rangle = |e1\rangle_{AB}|0\rangle_C$ ,  $|\phi_3\rangle = |11\rangle_{AB}|1\rangle_C$ ,  $|\phi_4\rangle = |1e\rangle_{AB}|0\rangle_C$ , and  $|\phi_5\rangle = |1a\rangle_{AB}|0\rangle_C$ . This evolution system is governed by the Hamiltonian

$$H_2 = \Omega_{0A}(t)|e\rangle_A\langle 0| + g_A|e\rangle_A\langle 1| + \Omega_{aB}(t)|e\rangle_B\langle a| + g_B|e\rangle_B\langle 1| + \text{H.c.} \quad (16)$$

By using the similar way to the above processes, the effective Hamiltonian of this system reads

$$H'_{\text{eff}} = \frac{1}{\sqrt{2}}|\mu\rangle(\Omega_{0A}(t)\langle\phi_1| + \Omega_{aB}(t)\langle\phi_5| + \text{H.c.}), \quad (17)$$

where  $|\mu\rangle = \frac{1}{\sqrt{2}}(-|\phi_2\rangle + |\phi_4\rangle)$ . To speed up the transition from  $|\phi_1\rangle$  to  $-|\phi_5\rangle$  by the invariant-based inverse engineering, we must find out the invariant Hermitian operator  $I(t)$  which satisfies (1). Since the effective Hamiltonian  $H'_{\text{eff}}$  possesses the  $\text{SU}(2)$  dynamical symmetry, the invariant  $I(t)$  can be given by [28]

$$I(t) = \frac{1}{\sqrt{2}}\chi(\cos\nu \sin\beta|\mu\rangle\langle\phi_1| + \cos\nu \cos\beta|\mu\rangle\langle\phi_5| + i \sin\nu|\phi_5\rangle\langle\phi_1| + \text{H.c.}), \quad (18)$$

where  $\chi$  is an arbitrary constant with units of frequency to keep  $I(t)$  with dimensions of energy. The time-dependent auxiliary parameters  $\nu$  and  $\beta$  satisfy the equations

$$\begin{aligned}\dot{\nu} &= \frac{1}{\sqrt{2}}(\Omega_{0A}(t) \cos \beta - \Omega_{aB}(t) \sin \beta), \\ \dot{\beta} &= \frac{1}{\sqrt{2}} \tan \nu (\Omega_{aB}(t) \cos \beta + \Omega_{0A}(t) \sin \beta).\end{aligned}\quad (19)$$

From (19) the expressions of  $\Omega_{0A}(t)$  and  $\Omega_{0B}(t)$  can be derived as follow

$$\begin{aligned}\Omega_{0A}(t) &= \sqrt{2}(\dot{\beta} \cot \nu \sin \beta + \dot{\nu} \cos \beta), \\ \Omega_{aB}(t) &= \sqrt{2}(\dot{\beta} \cot \nu \cos \beta - \dot{\nu} \sin \beta),\end{aligned}\quad (20)$$

where the dot denotes a time derivative. The eigenstates of the invariant  $I(t)$  are

$$\begin{aligned}|\Phi_0(t)\rangle &= \cos \nu \cos \beta |\phi_1\rangle - i \sin \nu |\mu\rangle - \cos \nu \sin \beta |\phi_5\rangle, \\ |\Phi_{\pm}(t)\rangle &= \frac{1}{\sqrt{2}}[(\sin \nu \cos \beta \pm i \sin \beta) |\phi_1\rangle + i \cos \nu |\mu\rangle \\ &\quad - (\sin \nu \sin \beta \mp i \cos \beta) |\phi_5\rangle],\end{aligned}\quad (21)$$

with the eugenvalues  $\varepsilon_0 = 0$  and  $\varepsilon_{\pm} = \pm 1$ , respectively. The solution of the Schrödinger equation  $i\hbar \frac{\partial |\Psi(t)\rangle}{\partial t} = H(t)|\Psi(t)\rangle$  can be written as the superposition of the eigenstates of  $I(t)$

$$|\Psi(t)\rangle = \sum_{n=0,\pm} C_n e^{i\alpha_n} |\Phi_n(t)\rangle, \quad (22)$$

where  $\alpha_n(t)$  is the Lewis-Riesenfeld phase in (3), and  $C_n$  is a time-independent amplitude. In order to get the final state  $-|\phi_5\rangle$ , we choose the parameters appropriately

$$\nu(t) = \epsilon, \quad \beta(t) = \frac{\pi t}{2t_f}, \quad (23)$$

where  $\epsilon$  is a time-independent small value. From the precise calculation, we can easily obtain

$$\begin{aligned}\Omega_{0A}(t) &= \frac{\pi}{\sqrt{2}t_f} \cot \epsilon \sin \frac{\pi t}{2t_f}, \\ \Omega_{aB}(t) &= \frac{\pi}{\sqrt{2}t_f} \cot \epsilon \cos \frac{\pi t}{2t_f}.\end{aligned}\quad (24)$$

When  $t = t_f$ ,

$$\begin{aligned}|\Psi(t_f)\rangle &= -\sin \epsilon \sin \alpha |\phi_1\rangle \\ &\quad + (-i \sin \epsilon \cos \epsilon + i \sin \epsilon \cos \epsilon \cos \alpha) |\mu\rangle \\ &\quad + (-\cos^2 \epsilon - \sin^2 \epsilon \cos \alpha) |\phi_5\rangle,\end{aligned}\quad (25)$$

where  $\alpha = \pi/(2 \sin \epsilon) = |\alpha_{\pm}|$ , and  $\alpha_{\pm}$  are the Lewis-Riesenfeld phases. As long as  $\alpha$  satisfies the condition  $\alpha = 2N\pi$  ( $N = 1, 2, 3, \dots$ ),  $|\Psi(t_f)\rangle = -|\phi_5\rangle = -|1a\rangle_{AB}|0\rangle_C$  can be achieved. Then the first step is realized successfully, and  $|\Psi_1\rangle = \alpha_{00}|00\rangle_{AB}|0\rangle_C - \alpha_{01}|1a\rangle_{AB}|0\rangle_C + \alpha_{10}|10\rangle_{AB}|0\rangle_C + \alpha_{11}|11\rangle_{AB}|0\rangle_C$  can be obtained.

The second step is just similar to the first step. In this step, the laser pulses are resonant with  $B$  atomic transition  $|0\rangle_B \leftrightarrow |e\rangle_B$  and  $A$  atomic transition  $|a\rangle_A \leftrightarrow |e\rangle_A$

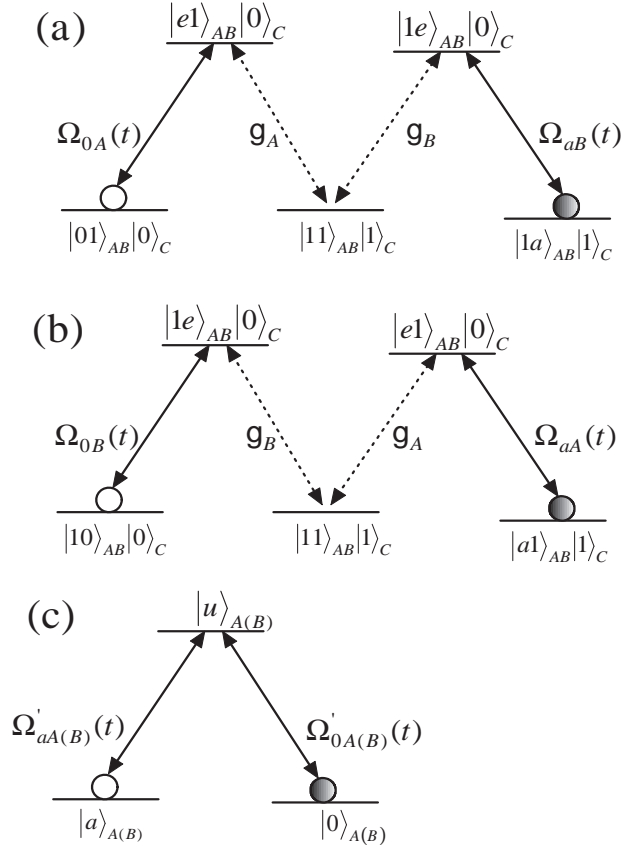


**Figure 2.** (Color online) The three steps for constructing the SWAP gate. For each step, the initial state is denoted by an empty circle and the final state is represented by a black circle.

with the corresponding Rabi frequencies  $\Omega_{0B}(t) = \frac{\pi}{\sqrt{2}t_f} \cot \epsilon \sin \frac{\pi t}{2t_f}$  and  $\Omega_{aA}(t) = \frac{\pi}{\sqrt{2}t_f} \cot \epsilon \cos \frac{\pi t}{2t_f}$ , respectively. In this step, the states  $|00\rangle_{AB}|0\rangle_C$ ,  $-|1a\rangle_{AB}|0\rangle_C$  and  $|11\rangle_{AB}|0\rangle_C$  will be remained the same, while the population of the state  $|10\rangle_{AB}|0\rangle_C$  is completely transferred to the state  $-|a1\rangle_{AB}|0\rangle_C$ , then  $|\Psi_2\rangle = \alpha_{00}|00\rangle_{AB}|0\rangle_C - \alpha_{01}|1a\rangle_{AB}|0\rangle_C - \alpha_{10}|a1\rangle_{AB}|0\rangle_C + \alpha_{11}|11\rangle_{AB}|0\rangle_C$  can be achieved.

The third step is just a one-qubit operation with the help of the auxiliary state  $|u\rangle_{A(B)}$ . The input laser pulses are resonant with  $A(B)$  atomic transition  $|0\rangle_{A(B)} \leftrightarrow |u\rangle_{A(B)}$  and  $|a\rangle_{A(B)} \leftrightarrow |u\rangle_{A(B)}$  with the corresponding Rabi frequencies  $\Omega'_{aA(B)}(t) = \frac{\pi}{\sqrt{2}t_f} \cot \epsilon \sin \frac{\pi t}{2t_f}$  and  $\Omega'_{0A(B)}(t) = \frac{\pi}{\sqrt{2}t_f} \cot \epsilon \cos \frac{\pi t}{2t_f}$ , respectively. The Hamiltonian in this step is given as follow

$$H_3 = \sum_{i=A,B} \Omega'_{ai}(t) |u\rangle_i \langle a| + \Omega'_{0i}(t) |u\rangle_i \langle 0| + \text{H.c.} \quad (26)$$

For the initial atomic state  $|a\rangle_{A(B)}$ , the population will finally transfer to the state  $-|0\rangle_{A(B)}$  by using the similar way in the first step. Thus, we can obtain  $|\Psi_3\rangle = \alpha_{00}|00\rangle_{AB}|0\rangle_C + \alpha_{01}|10\rangle_{AB}|0\rangle_C + \alpha_{10}|01\rangle_{a1}|0\rangle_C + \alpha_{11}|11\rangle_{AB}|0\rangle_C$ . That is the result of the SWAP gate. figure 2 represents these three steps for constructing the SWAP gate.

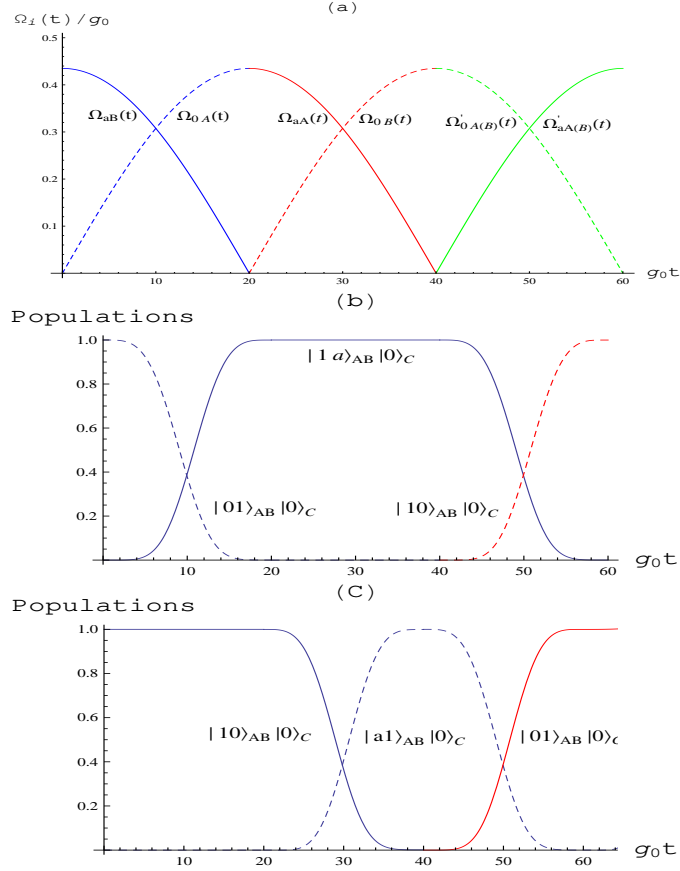


**Figure 3.** (Color online) (a) Temporal profile of the time dependence Rabi frequencies  $\Omega_i(t)/g_0$  versus  $t/g_0$  with  $\Omega_i(t) = \Omega_{0A}(t)$  (dash blue line),  $\Omega_{aB}(t)$  (solid blue line),  $\Omega_{0B}(t)$  (dash red line),  $\Omega_{aA}(t)$  (solid red line),  $\Omega'_{aA(B)}(t)$  (solid green line),  $\Omega'_{0A(B)}(t)$  (dash green line). (b) Time evolutions of the populations of the corresponding system states with the initial states  $|01\rangle$ . (c) Time evolutions of the populations of the corresponding system states with the initial state  $|10\rangle$ . The system parameters are set to be  $\epsilon = 0.25$ ,  $g_A = g_B = 10g_0$  and  $t_f = 20/g_0$ .

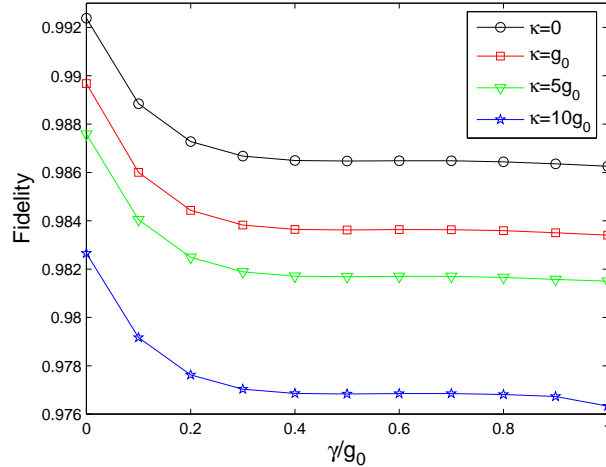


**Figure 4.** (Color online) The effect of atomic spontaneous emission  $\gamma$  on the fidelity of the SWAP gate with different values of the cavity decay  $\kappa$ .



#### 4. Numerical simulations and feasibility analysis

In the following, we make the numerical simulations to verify the validity of the SWAP gate. figure 3(a) shows the time-dependence laser pulse  $\Omega_m(t)/g_0$  as a function of  $t/g_0$  for a fixed value  $\epsilon = 0.25$ ,  $g_A = g_B = 10g_0$  and  $t_f = 20/g_0$ . With these parameters, the Zeno condition can be met well. The populations of the states  $|01\rangle_{AB}|0\rangle_C$  and  $|10\rangle_{AB}|0\rangle_C$  swap perfectly which can be seen from figure 3(a) and figure 3(b). Whether a scheme is available largely depends on the robustness to the loss and decoherence, so in the following, we consider the loss and decoherence effects on our SWAP gate operation. The corresponding master equation for the whole system density matrix  $\rho(t)$  has the following form:

$$\begin{aligned} \dot{\rho}(t) = & -i[H_{\text{total}}, \rho(t)] - \frac{\kappa}{2}[a^\dagger a \rho(t) - 2a \rho(t) a^\dagger + \rho(t) a^\dagger a] \\ & - \frac{\gamma_A}{2} \sum_{l=e,u} \sum_{k=0,1,a} [\sigma_{l,l}^A \rho(t) - 2\sigma_{k,l}^A \rho(t) \sigma_{l,k}^A + \rho(t) \sigma_{l,l}^A] \\ & - \frac{\gamma_B}{2} \sum_{l=e,u} \sum_{k=0,1,a} [\sigma_{l,l}^B \rho(t) - 2\sigma_{k,l}^B \rho(t) \sigma_{l,k}^B + \rho(t) \sigma_{l,l}^B], \end{aligned} \quad (27)$$

where  $H_{\text{total}} = H_1 + H_2 + H_3$ .  $\kappa$  is the cavity decay rate,  $\gamma_{A(B)}$  is  $A(B)$  atomic spontaneous emission rate from the excited state  $|l\rangle_i (l = e, u; i = A, B)$  to the ground state  $|k\rangle_i (k = 0, 1, a)$ , respectively.  $\sigma_{l,k} = |l\rangle \langle k|$ . For simplicity, we assume  $\gamma_A = \gamma_B = \gamma$  and the initial condition  $\rho(0) = |\Psi_0\rangle \langle \Psi_0|$ . In figure 4, the fidelity of the SWAP gate is plotted versus the dimensionless parameter  $\gamma/g$  with different values of  $\kappa/g_0$  by numerically solving the master (27). From figure 4 we can see that the fidelity of our SWAP gate is higher than 97.6% even when the values of  $\gamma$  and  $\kappa$  are comparable to  $\gamma = 0.1g_{A(B)} = g_0$  and  $\kappa = g_{A(B)} = 10g_0$ . It shows that the SWAP gate in our scheme is robust against decoherence due to cavity decay and atomic spontaneous emission.

Now we give a brief analysis of the feasibility in experiment for this scheme. The scheme can be realized with trapped ions and nitrogen-vacancy color center in diamond [29], cavity QED systems [30, 31, 32] or with impurity levels in a solid, such as  $\text{Pr}^{3+}$  ions in  $\text{Y}_2\text{SiO}_5$  crystal [33]. In recent experiments, the fabrication of various high-Q microcavities including whispering-gallery-mode cavities [34, 35], micropost cavities, and one- or two-dimensional photonic-crystal microcavities [36, 37] also have been well designed. And the suitable parameters of toroidal microcavity system for strong-coupling cavity QED have been investigated and the parameters can be chosen as  $(g, \kappa, \gamma)/2\pi = (750, 3.5, 2.62)$  MHz [35]. In this case,  $\gamma \simeq 0.0034g_{A(B)} = 0.034g_0$ ,  $\kappa \simeq 0.0046g_{A(B)} = 0.046g_0$ , and with these parameters the fidelity of SWAP gate can reach 99%. So our scheme is robust against both the cavity decay and atomic spontaneous emission and could be very promising and useful for quantum information processing.

## 5. Conclusion

In summary, we have proposed a promising scheme to implement a SWAP gate through the shortcut to adiabatic passage and QZD instead of relying on the compositions of a large number of elementary gates. We also study the influences of atomic spontaneous emission and cavity decay on the fidelity through numerical simulation. The numerical simulation results denote that our scheme is very robust against the decoherence caused by atomic spontaneous emission and cavity decay, so it can be a more reliable choice in experiment. We believe that our scheme will be useful to realize quantum algorithms, such as Shor's algorithm for prime factoring or Grover's algorithm for database search.

## Acknowledgments

This work was supported by the National Natural Science Foundation of China under Grant Nos. 11464046, 11264042, 11465020 and 61465013.

## References

- [1] Huang Y F, Ren X F, Zhang Y S, Duan L M and Guo G C 2004 *Phys. Rev. Lett.* **93** 240501
- [2] Qiao B, Ruda H E and Wang J 2002 *J. Appl. Phys.* **91** 2524
- [3] Cui W X, Hu S, Wang H F, Zhu A D and Zhang S 2015 *Laser Phys. Lett.* **24** 045204
- [4] Zheng S B 2013 *Phys. Rev. A* **87** 042318
- [5] Cirac J I and Zoller P 1995 *Phys. Rev. Lett.* **74** 4091
- [6] Šašura M and Bužek V 2001 *Phys. Rev. A* **64** 012305
- [7] Yang C P, Chu Shih-I and Han S 2003 *Phys. Rev. A* **67** 042311
- [8] Wineland D J and Leibfried D 2011 *Laser Phys. Lett.* **8** 175
- [9] Yang C P and Han S 2006 *Phys. Rev. A* **73** 032317
- [10] Kuklinski J R, Gaubatz U, Hioe F T and Bergmann K 1989 *Phys. Rev. A* **40** 6741
- [11] Ruschhaupt A, Chen X, Alonso D and Muga J G 2012 *New J. Phys.* **14** 093040
- [12] Chen X, Lizuain I, Ruschhaupt A, Guéry-Odelin D and Muga J G 2010 *Phys. Rev. Lett.* **105** 123003
- [13] Hoffmann K H, Salamon P, Rezek Y and Kosloff R 2011 *Europhys. Lett.* **96** 60015
- [14] del Campo A 2013 *Phys. Rev. Lett.* **111** 100502
- [15] Lu M, Xia Y, Shen L T, Song J and An N B 2014 *Phys. Rev. A* **89** 012326
- [16] Chen Y H, Xia Y, Chen Q Q and Song J 2014 *Phys. Rev. A* **89** 033856
- [17] Walther A, Ziesel F, Ruster T, Dawkins S T, Ott K, Hettrich M, Singer K, Schmidt-Kaler F and Poschinger U 2012 *Phys. Rev. Lett.* **109** 080501
- [18] Schaff J F, Song X L, Capuzzi P, Vignolo P and Labeyrie G 2011 *Europhys. Lett.* **93** 23001
- [19] Cheng Y H, Xia Y, Chen Q Q and Song J 2015 *Phys. Rev. A* **91** 012325
- [20] del Campo A, Rams M M, Zurek W H 2012 *Phys. Rev. Lett.* **109** 115703
- [21] Saberi H, Opatrný T, Mølmer K, del Campo A 2014 *Phys. Rev. A* **90** 060301(R)
- [22] Liang Y, Wu Q C, Su S L, Ji X and Zhang S 2015 *Phys. Rev. A* **91** 032304
- [23] Kwiat P, Weinfurter H, Herzog T, Zeilinger A and Kasevich M A 1995 *Phys. Rev. Lett.* **74** 4763
- [24] Facchi P, Gorini V, Marmo G, Pascazio S and Sudarshan E C G 2000 *Phys. Lett. A* **275** 12
- [25] Lewis H R and Riesenfeld W B 1969 *J. Math. Phys.* **10** 1458
- [26] Lohe M A 2009 *J. Phys. A: Math. and Theor.* **42** 035307
- [27] Misra B, Sudarshan E C G 1977 *J. Math. Phys.* **18** 756
- [28] Chen X, Torrontegui E and Muga J G 2011 *Phys. Rev. A* **83** 062116

- [29] Shahriar M S, Hemmer P R, Lloyd S, Bhatia P S and Craig A E 2002 *Phys. Rev. A* **66** 032301
- [30] Schneider S, James D F V and Milburn G J 2000 *J. Mod. Opt.* **47** 499
- [31] Pachos J and Walther H 2002 *Phys. Rev. Lett.* **89** 187903
- [32] You L, Yi X X and Su X H 2003 *Phys. Rev. A* **67** 032308
- [33] Ichimura K 2001 *Opt. Commun.* **196** 119
- [34] Armani D K, Kippenberg T J, Spillane S M and Vahala K J 2003 *Nature* **421** 925
- [35] Spillane S M, Kippenberg T J, Vahala K J, Goh K W, Wilcut E and Kimble H J 2005 *Phys. Rev. A* **71** 013817
- [36] Song B S, Noda S, Asano T and Akahane Y 2005 *Nature Mater.* **4** 207
- [37] Tanabe T, Notomi M, Kuramochi E, Shinya A and Taniyama H 2007 *Nature Photon.* **1** 49